Dalton Transactions

PAPER

View Article Online
View Journal | View Issue

Cite this: *Dalton Trans.*, 2023, **52**, 16492

Mechanistic insights into nitric oxide oxygenation (NOO) reactions of $\{CrNO\}^5$ and $\{CoNO\}^8$†

Akshaya Keerthi C. S.,[a] Sandip Das,[a] Kulbir,[a] Prabhakar Bhardwaj,[a] Md Palashuddin Sk[b] and Pankaj Kumar *[a]

Received 27th September 2023,
Accepted 13th October 2023

DOI: 10.1039/d3dt03177b

rsc.li/dalton

Here, we report the nitric oxide oxygenation (NOO) reactions of two distinct metal nitrosyls {Co–nitrosyl (S = 0) *vs.* Cr–nitrosyl (S = 1/2)}. In this regard, we synthesized and characterized $[(BPMEN)Co(NO)]^{2+}$ ($\{CoNO\}^8$, **1**) to compare its NOO reaction with that of $[(BPMEN)Cr(NO)(Cl^-)]^+$ ($\{CrNO\}^5$, **2**), having a similar ligand framework. Kinetic measurements showed that $\{CrNO\}^5$ is thermally more stable than $\{CoNO\}^8$. Complexes **1** and **2**, upon reaction with the superoxide anion ($O_2^{\bullet-}$), generate $[(BPMEN)Co^{II}(NO_2^-)_2]$ ($Co^{II}–NO_2^-$, **3**) and $[(BPMEN)Cr^{III}(NO_2^-)Cl^-]^+$ ($Cr^{III}–NO_2^-$, **4**), respectively, with O_2 evolution. Furthermore, analysis of these NOO reactions and tracking of the N-atom using ^{15}N-labeled NO (^{15}NO) revealed that the N-atoms of **3** ($Co^{II}–^{15}NO_2^-$) and **4** ($Cr^{III}–^{15}NO_2^-$) derive from the nitrosyl (^{15}NO) moieties of **1** and **2**, respectively. This work represents a comparative study of oxidation reactions of $\{CoNO\}^8$ *vs.* $\{CrNO\}^5$, showing different rates of the NOO reactions due to different thermal stability. To complete the NOM cycle, we reacted **3** and **4** with NO, and surprisingly, only **3** generated $\{CoNO\}^8$ species, while **4** was unreactive towards NO. Furthermore, the phenol ring nitration test, performed using 2,4-di-*tert*-butylphenol (2,4-DTBP), suggested the presence of a proposed peroxynitrite (PN) intermediate in the NOO reactions of **1** and **2**.

Introduction

Nitric oxide (NO) is a simple gas earlier thought to be an atmospheric pollutant and poison.[1] In recent years, NO has been proven to be one of the essential signaling gases participating in a wide range of physiological processes, *i.e.*, neurotransmission, vascular regulation, disaggregation of platelets, immune response towards multiple infections, *etc.*[1,2] Inadequate NO generation causes biological dysfunctions (*vide supra*) and causes various diseases, such as diabetic hypertension,[3] kidney disease,[3] atherosclerosis,[4] cognitive dysfunctions,[5] *etc.*[6] Hence, to maintain biological homeostasis, two families of biological enzymes, *i.e.*, nitric oxide synthases (NOSs)[7,8] and nitrite reductases (NiRs),[9] are involved in NO biosynthesis. When overproduced, NO leads to cytotoxicity by forming reactive nitrogen species (RNS), *i.e.*, peroxynitrite (PN, $OONO^-$)[10] and nitrogen dioxide ($^{\bullet}NO_2$),[11] upon reaction with dioxygen (O_2),[12] the superoxide anion ($O_2^{\bullet-}$),[13] or hydrogen peroxide (H_2O_2).[14] Thus, maintaining the optimal level of NO in the biosystem is necessary. Therefore, microbial/or mammalian systems oxidize excess NO to biologically benign nitrate (NO_3^-) using Fe-containing nitric oxide dioxygenase (NOD)[15] enzymes *via* a plausible PN intermediate.[16] In some bacteria and archaea, a unique di-iron protein carries out the process of NO detoxification by reducing it into N_2O.[17]

Bio-mimetic modeling of NOD enzymes and their mechanistic investigation proposed the formation of a metal–dioxygen adduct upon reaction with O_2, which then reacts with NO to generate NO_3^- *via* a proposed M–PN intermediate.[15b,18] Several models of metal–dioxygen (M–O_2) intermediates were developed to understand/establish the actual mechanism of the NOD reaction.[19] In this regard, Kurtikyan *et al.* studied oxycoboglobin's NOD reaction that generates Co–NO_3^- at low temperatures.[20] Also, $Cr^{IV}–O_2^{2-}$ and $Co^{III}–O_2^{2-}$ species produced $Cr^{III}–NO_3^-$ and $Co^{II}–NO_3^-$ species when reacted with NO, respectively.[19c,21] In addition to NOD reaction products, NO-monooxygenation (NOM) products were also observed in several metal–dioxygen adduct reactions with NO. Karlin and coworkers observed $Cu^{II}–NO_2^-$ in the reaction of $Cu^{II}–O_2^{\bullet-}$ with NO *via* a PN intermediate.[22] Nam and coworkers observed a NOM product formation ($Cr^{III}–NO_2^-$) in the reaction of $Cr^{III}–O_2^{\bullet-}$ with NO *via* a $Cr^{IV}{=}O$ species.[19b] Contrarily, the reaction

[a]Department of Chemistry, Indian Institute of Science Education and Research (IISER), Tirupati 517507, India. E-mail: pankajatiisert@gmail.com, pankaj.iisertirupati@gmail.com
[b]Department of Chemistry, Aligarh Muslim University (AMU) Aligarh, Uttar Pradesh 202001, India

†Electronic supplementary information (ESI) available. CCDC 2206431 and 2206432. For ESI and crystallographic data in CIF or other electronic format see DOI: https://doi.org/10.1039/d3dt03177b

of $Fe–O_2^{2-}$ with NO^+ led to an $Fe^{III}–NO_3^-$ complex, a NOD reaction product.[19a] In another case, $Fe–O_2^{•-}$ and $Mn–O_2^{2-}$ bearing the TAML ligand led to the formation of $Fe^{III}–NO_3^-$ and $Mn^{IV}{=}O + NO_2$ *via* a presumed PN intermediate, respectively.[23] Thus, the metal center considerably controls the NO oxygenation reaction (NOD *vs.* NOM). In this regard, several comparative studies were performed to understand the role of the metal center. Recently, we have studied the comparative NO oxygenation reactivity of $Co–O_2^{2-}$ and $Ni–O_2^{2-}$ bearing a similar 12TMC ligand framework that generates $Co^{II}–NO_2^-$ and $Ni^{II}–NO_3^-$ as the end products.[24] Groves and coworkers reported the formation of $Fe^{IV}{=}O$ and NO_2 in the reaction of metHb with the PN molecule.[25] Considerable work is underway and has also already been performed to establish the presence of a PN intermediate in NO oxidation reactions, *i.e.*, IR,[19f,20,26] EPR,[19f] *etc.*; however, the same is under debate. In contrast, Pacheco and the group proposed that the NOD reaction with oxymyoglobin does not share the PN intermediate.[27] Further supported by Moënne-Loccoz and coworkers' work on the NOD reaction of oxymyoglobin, it is portentous that the millisecond intermediate is an $Fe^{III}–NO_3^-$ species and not a PN intermediate.[28] Although the PN intermediate was not detected in the oxy-globin protein's NOD reaction, the experimental results proposed a short-lifetime intermediate before forming metal–NO_3^-.[19e] In biology, an additional pathway of the NOD reaction has also been presented, which suggests Fe–NO formation upon reaction of NO with the Fe-center of Hb, and then it reacts with O_2, resulting in NO_3^- formation.[29] However, a reverse pathway was investigated in detail by Stuehr and coworkers by taking a series of different Fe–NO species.[30]

Hence, the NO activation using metal ions has been an active field of research for chemists and biochemists for many years to understand its coordination chemistry and reactivity.[31] In various biological enzymatic reactions, *i.e.*, nitrogen fixation,[32] NiR reaction,[24,33] NOD reactions,[15a,34] *etc.*, M–NOs are the key intermediates. In recent years, very few M–NOs have been prepared and explored for their various reactions to understand and mimic the biological M–NOs' reactivity.[15c,31-d,35] Among them, only a few M–NOs were examined for NO-oxidation reactions, *i.e.*, reactions with dioxygen,[12] superoxides,[13] base,[36] and H_2O.[37] Oxidation of M–NOs generates NO mono- or di-oxygenated products, usually depending on the type of M–NO and stability of the intermediate involved. $\{CoNO\}^8$ produced NO_2^- when reacted with O_2;[38] in another example, $\{FeNO\}^7$ formed NO_2^- from NO oxidation.[39] Recently, Nam and coworkers showed the oxidation of $\{CoNO\}^8$ to $Co^{II}–NO_3^-$ and $Co^{II}–NO_2^- + O_2$ upon reaction with O_2 and $O_2^{•-}$, respectively.[35b] Also, Mondal and coworkers reported the NO_3^- generation from $\{CoNO\}^8$ and $\{CuNO\}^{10}$ species upon reaction with hydrogen peroxide (H_2O_2) *via* a proposed PN intermediate.[40] In contrast to $\{CoNO\}^8$ reactivity towards $O_2^{•-}$, $\{MnNO\}^6$ upon reaction with $O_2^{•-}$ generated $Mn^{III}–NO_3^-$ *via* a presumed PN intermediate.[41] As the oxidized products of M–NOs depend upon the choice of the metal center, their oxidation state, and the intermediate involved in the reaction, a deep study is required to establish the actual mechanism of the M–NO oxidation reactions.

Among various metal–nitrosyl complexes, $\{CrNO\}^5$ and $\{CoNO\}^8$ species are widely explored and known to be reasonably stable with linear and bent metal–NO coordination, respectively.[24,33e,35b,42] Thus, to understand the NO oxidation reactions of metal–nitrosyl complexes, we prepared $\{CrNO\}^5$ ($S = 1/2$) and $\{CoNO\}^8$ ($S = 0$), having different spin states/magnetic properties with similar ligand frameworks. Therefore, $[(BPMEN)Co(NO)]^{2+}$ ($\{CoNO\}^8$, **1**) and $[(BPMEN)Cr(NO)(Cl^-)]^+$ ($\{CrNO\}^5$, **2**) complexes[43] (BPMEN = *N*,*N*′-bis(2-pyridylmethyl)-1,2-diaminoethane) were explored for their reactivity towards $O_2^{•-}$ (KO_2/18-crown-6), to understand the effect of the metal center and the spin state/magnetic properties (Scheme 1). Following our previous reports,[43,44] we synthesized new $\{CoNO\}^8$ and $\{CrNO\}^5$ complexes and calculated various physical parameters for **1** and **2** to determine their thermal stability, the NO oxidation reactions and the intermediates involved (Scheme 1, reactions a and b). Complex **1** generates a Co^{II}–nitrito complex $[(BPMEN)Co^{II}(NO_2^-)_2]$ ($Co^{II}–NO_2^-$, **3**) + O_2 in the presence of $O_2^{•-}$ *via* a proposed thermally unstable $[Co–PN]^+$ species (Scheme 1, reaction c). However, **2** generates an oxidized Cr^{III}–nitrito complex $[(BPMEN)Cr^{III}(NO_2^-)Cl^-]^+$ ($Cr^{III}–NO_2^-$, **4**) + O_2 upon reaction with $O_2^{•-}$ *via* a proposed $[Cr–PN]^+$ intermediate species (Scheme 1, reaction d). The phenol ring nitration test performed using 2,4-DTBP suggested the presence of the proposed PN intermediate in the NOM reactions of **1** and **2**. Mechanistic studies using ^{15}N-labeled nitric oxide (^{15}NO) revealed that the N-atoms of **3** ($Co^{II}–^{15}NO_2^-$) and **4** ($Cr^{III}–^{15}NO_2^-$) were derived from the ^{15}NO moieties of **1** and **2**, respectively. In addition, to complete the NOM cycle, we reacted **3** and **4** with NO, which showed the formation of $\{CoNO\}^8$ from **3**, while **4** was unreactive to NO (Scheme 1, reactions e and f). The equilibrium constant (K_{eq}) of the formation of **2** is ∼25 times that of **1**, suggesting that **2** is more stable than **1**; hence, it also explains why the reaction of **2** with $O_2^{•-}$ is slower than that of **1**. In both reactions, we observed NO_2^- (NOM) formation; however, only complex **3** could generate the initial M–NO (**1**) while **4** was unreactive towards NO.

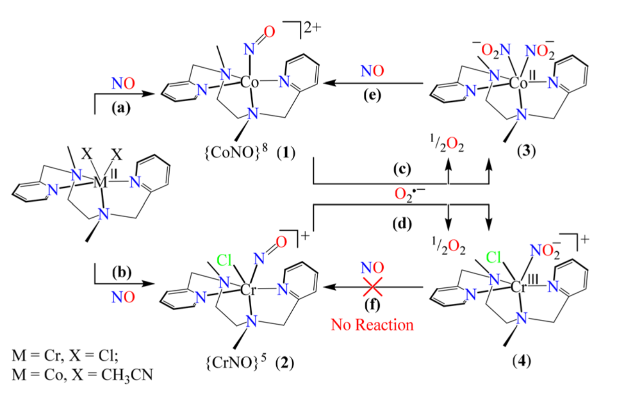

Scheme 1 NO activation at Cr and Co centers and NOO reactions of **1** and **2**.

Results and discussion

Synthesis of Co–nitrosyl, $[(BPMEN)Co(NO)]^{2+}$ ($\{CoNO\}^8$, 1)

The initial Co^{II}-complex $[(BPMEN)Co^{II}(CH_3CN)_2]^{2+}$ (Co-**1**) was synthesized by adding the BPMEN ligand to a stirring solution of $[Co^{II}(H_2O)_6](BF_4)_2$ and characterized with various spectroscopic measurements (Fig. 2, see the ESI and Experimental section (ES), Fig. S1†). The addition of excess NO to the CH_3CN solution of Co-**1** at 233 K under an Ar atmosphere resulted in the generation of $[(BPMEN)Co(NO)]^{2+}$ ($\{CoNO\}^8$, **1**) (λ_{max} = 375, ε = 956 M^{-1} cm^{-1}, red line) within one hour (Fig. 1a and ESI Fig. S2a†) (Scheme 1, reaction a). The FT-IR spectrum also reveals that the NO moiety is bound to a Co-center, suggesting a bent NO with a typical Co–NO stretching at 1653 cm^{-1} (inset: Fig. 1a; ESI, Fig. S2b†).[33e,35a,b] Electrospray ionization mass spectrometry (ESI-MS) of **1** showed a prominent ion peak at *m/z* 376.1, whose mass and isotope distribution patterns correspond to $[(BPMEN)Co(NO)(OH^-)]^+$ (calcd *m/z* 376.1) (ESI,† Fig. 1b). Upon substitution of the NO moiety with ^{15}N-labeled ^{15}NO in **1**,[24,45] the mass peak corresponding to $[Co(BPMEN)(^{15}NO)(OH^-)]^+$ appears at *m/z* 377.1 (calcd *m/z* 377.1) (inset: Fig. 1b; ESI, Fig. S2c†), suggesting that the NO moiety is bound to the Co-center. The Evans' method established a high-spin Co^{II}-center (S = 3/2) in Co-**1** (ESI, Fig. S1e†);[46] hence, its ^1H NMR does not show any signal for aromatic/aliphatic protons in the normal range (ESI, Fig. S3a†). However, we observed these signals in complex **1**, confirming a diamagnetic Co-center (ESI, Fig. S3b†). The redox potential of **1** was determined using a cyclic voltammogram (ESI, Fig. S3c†). To perform NOO experiments, we prepared/isolated **1** by purging Co-**1** with excess NO gas in CH_3CN at 233 K under Ar (ESI, ES;† yield: 76%).

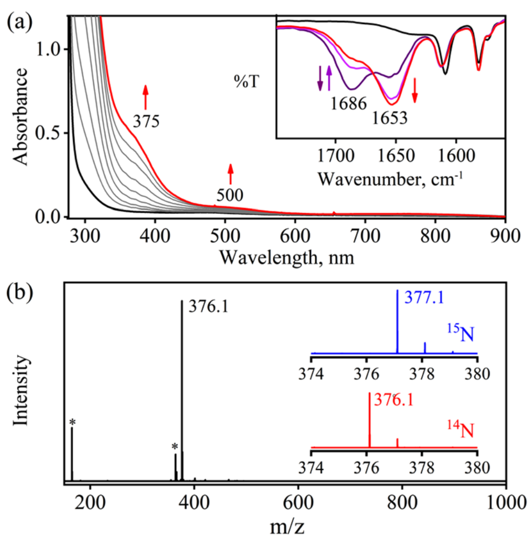

Fig. 1 (a) UV-vis spectral change of Co-**1** (0.5 mM, black line) upon addition of $NO_{(g)}$ in CH_3CN under Ar at 233 K. Inset: Solution IR spectra of the formation of **1** (red line). (b) ESI-MS spectra of **1**. The peak at 376.1 is assigned to $[(BPMEN)Co^{II}(NO)(OH^-)]^+$ (calcd *m/z* 376.1). Inset: Isotopic distribution patterns of **1**-^{14}NO (red line) and **1**-^{15}NO (blue line). The peaks at *m/z* 364.1 and 164.5 marked with asterisks are assigned to $[(BPMEN)Co(Cl^-)]^+$ and $[(BPMEN)Co]^{2+}$, respectively.

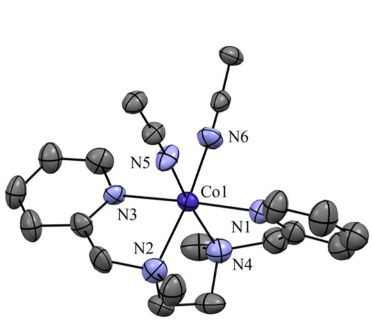

Fig. 2 Displacement ellipsoid plot (30% probability) of Co-**1** at 298 K. Anions and H-atoms have been removed for clarity.

NO oxygenation reaction of the $\{CoNO\}^8$ complex (1)

To explore the NO oxygenation (NOO) reaction of $\{CoNO\}^8$, we reacted the new Co–NO complex $[(BPMEN)Co(NO)]^{2+}$ ($\{CoNO\}^8$, **1**; S = 0) with $O_2^{\bullet-}$. The addition of $O_2^{\bullet-}$ to a solution of **1** resulted in the generation of $[(BPMEN)Co^{II}(NO_2^-)_2]$ (Co^{II}–NO_2^-, **3**). The characteristic UV-vis absorption bands of **1** (λ_{max} = 375 nm, ε = 956 M^{-1} cm^{-1}) changed to a new band (λ_{max} = 360 nm, ε = 4040 M^{-1} cm^{-1}), which corresponds to **3**, within 5 minutes in CH_3CN at 298 K under Ar (Fig. 3a; ESI, Fig. S5†). However, **1** does not show any spectral changes in the absence of $O_2^{\bullet-}$, ruling out the natural decomposition of **1** generating free NO followed by the reaction with $O_2^{\bullet-}$ (ESI, Fig. S5b†). Complex **3** was determined to be $[(BPMEN)Co^{II}(NO_2^-)_2]$ based on various spectroscopic and single-crystal X-ray structural

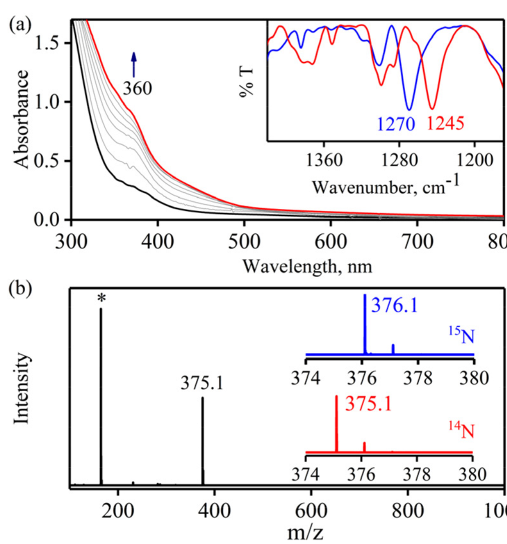

Fig. 3 (a) UV-vis spectral change of **1** (0.25 mM, black line) upon addition of KO_2/18-crown-6 in CH_3CN under Ar at 298 K. Inset: IR spectra of **3**-$^{14}NO_2^-$ (blue line) and **3**-$^{15}NO_2^-$ (red line) in KBr. (b) ESI-MS spectra of **3**. The peak at 375.1 is assigned to $[(BPMENCo(NO_2^-)]^+$ (calcd *m/z* 375.1). Inset: Isotopic distribution patterns of **3**-$^{14}NO_2^-$ (red line) and **3**-$^{15}NO_2^-$ (blue line).

analyses (*vide infra*). The FT-IR spectrum of **3** showed a characteristic peak for Co^{II}-bound NO_2^- stretching at 1270 cm^{-1}, which shifted to 1245 cm^{-1} ($^{15}NO_2^-$) when **3** was generated in the reaction of ^{15}N-labeled NO $\{Co^{15}NO\}^8$ and $O_2^{\bullet-}$ (inset: Fig. 3a; ESI, Fig. S6a and b†), suggesting that the N-atom in the $^{15}NO_2^-$ moiety is derived from $\{Co^{15}NO\}^8$. The ESI-MS spectrum of **3** showed a prominent peak at *m*/*z* 375.1, $[(BPMEN)Co(^{14}NO_2^-)]^+$ (calcd *m*/*z* 375.1), which shifted to 376.1, $[(BPMEN)Co(^{15}NO_2^-)]^+$ (calcd *m*/*z* 376.1), when the reaction was performed using $\{Co^{15}NO\}^8$ (Fig. 3b; ESI, Fig. S7†), indicating that the NO_2^- derived from the NO moiety of **1**. We did not observe the characteristic signal of aliphatic protons of the BPMEN ligand for **3** in the ^{1}H-NMR spectrum, signifying a bivalent cobalt center.[35a,45c] In addition, Evans' method confirmed a low-spin Co^{II}-center (S = 1/2), as the magnetic moment of **3** was found to be 1.77 BM (ESI; ES, Fig. S8†).[46] Electrochemical measurement of **3** showed a non-reversible cyclic voltammogram (ESI, Fig. S9†). The exact conformation of **3** was determined by single-crystal X-ray crystallographic structural analysis (Fig. 4a, ESI, ES, and Tables T1 and T2†). The two NO_2^- ligands are coordinated to a Co-center in an end-on fashion with a distorted octahedral geometry. The Co–O–N and O–N–O bond angles were 118.91 and 116.12, respectively. The Griess reagent test confirmed the amount of NO_2^- generated in the above reaction and was determined to be 93 (±5)% (ESI; SI, Fig. S10†).[35a,47] Various spectral and structural analyses of **3** undoubtedly showed that the reaction of **1** with $O_2^{\bullet-}$ generated Co^{II}–NO_2^- (**3**) as the NOM product (Scheme 1c). The side product of the NOM reaction of **1** was determined to be O_2, which is believed to be formed *via* a proposed transient $[Co–PN]^+$ intermediate (Scheme 2). The PN intermediate is known to be a source of the reactive oxygen atom, which can produce O_2;[35a] also, in an aqueous medium, PN was found to generate the NO_2^- anion with O_2.[48] Recently, one of our reports on the Co^{III}–peroxo reaction with NO showed the generation of NO_2^- + O_2 *via* a $[Co–PN]^+$ intermediate,[24] and similarly Nam and coworkers demonstrated the formation of Co^{II}–NO_2^- and O_2 *via* a $[Co–PN]^+$ intermediate.[35a] Likewise, the generation of Cu^{II}–NO_2^- with the evolution of O_2 was observed from a $[Cu–PN]^+$ intermediate.[22,49] Hence, in the above reaction, the generation of Co^{II}–NO_2^- with O_2 evolution supports our assumption of the proposed $[Co–PN]^+$ intermediate, as described in the previous reports on aqueous PN chemistry,[48] non-aqueous Co^{II}–PN,[35a] and Cu^{II}–PN[22,49] chemistry. We followed and trapped the evolved O_2 by following its generation from the reaction solution to support our assumption as proposed in $[Co–PN]^+$ chemistry[19f,20,26] and aqueous PN chemistry.[48] To confirm the formation of O_2, we carried out the reaction of **1** with $O_2^{\bullet-}$ and followed the generation of gases by reaction flask headspace analysis using a gas-mass analyzer and observed the formation of O_2 (Fig. 4b). In addition, we attempted to characterize the proposed $[Co–PN]^+$ intermediate to elucidate the mechanism of its conversion to **3** in the above NOM reaction (Scheme 2). However, our efforts to characterize the $[Co–PN]^+$ were futile due to its unstable nature. However, indirectly, the PN intermediate was detected by a DTBP ring-nitration test, as reported in the previous literature[19c,f,41,42c] and as explained in the chemistry we have described earlier (*vide supra*).[12] The generation of NO_2-2,4-DTBP (~52%) and 2,4-DTBP-D (~12%) (ESI, Fig. S11†) actively supports the proposed reaction mechanism in the above NOM reaction and, therefore, the formation of a $[Co–PN]^+$ intermediate in the reactions of **1** with $O_2^{\bullet-}$ (Scheme 2, reactions a and b). The formation of a $[Co(BPMEN)(NO)(O_2^{\bullet-})]^+$ species before PN formation, as reported earlier, can't be ruled out,[42c,50] but such an intermediate further undergoes rearrangement to generate the PN intermediate ultimately. We did not observe the formation of such species spectroscopically; however, indirect proof from the phenol ring nitration test confirms the PN formation.

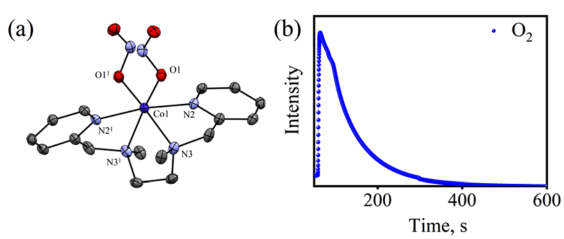

Fig. 4 (a) Displacement ellipsoid plot (30% probability) of **3** at 100 K. H-atoms have been removed for clarity. (b) Mass spectra of the formation of O_2 in the reaction of **1** (20.0 mM) with $O_2^{\bullet-}$.

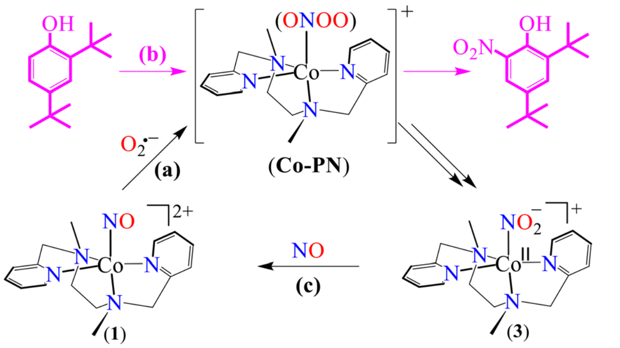

Scheme 2 Phenol ring nitration to trap the $[Co–PN]^+$ intermediate.

NO oxygenation reaction of the $\{CrNO\}^5$ complex (2)

In order to find the influence of the metal center on oxidation of metal-bound nitrosyls, we explored the reaction of $[(BPMEN)Cr(NO)(Cl^-)]^+$ ($\{CrNO\}^5$, **2**) with $O_2^{\bullet-}$ (yield: 70%). Complex **2** was synthesized and isolated by following our previous report.[43] The addition of one equivalent of $O_2^{\bullet-}$ (KO_2/18-crown-6) to a CH_3CN solution of **2** under Ar showed a color change from light green to dark red at 298 K. Upon reaction of **2** with $O_2^{\bullet-}$, the characteristic UV-vis absorption bands of **2** (black line, λ_{max} = 600 nm) changed to a new band (blue line, λ_{max} = 450 nm) within ~one minute (Fig. 5a), which gradually changed to the red line (NO-oxidized product, **4**) in ~five minutes (Fig. 5a, ESI, Fig. S12a†) at 298 K under an Ar atmo-

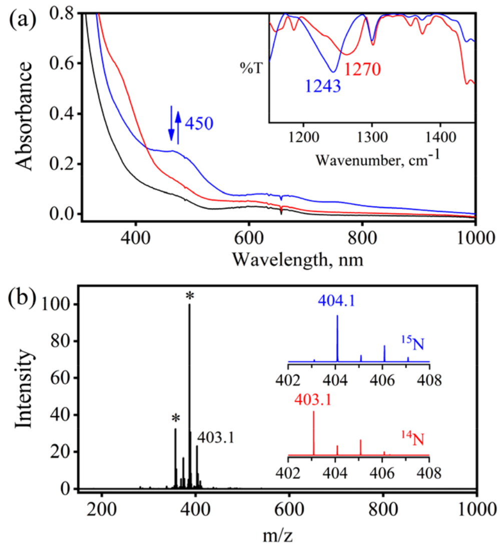

Fig. 5 (a) UV-vis spectral change of **2** (1 mM, black line) upon addition of KO_2/18-crown-6 showing the formation of the blue line, and it further decomposes to form **4** (red line) in CH_3CN under Ar at 298 K. Inset: IR spectra of **4**-$^{14}NO_2^-$ (red line) and **4**-$^{15}NO_2^-$ (blue line) in KBr. (b) ESI-MS of **4** formed in the reaction of **2** with KO_2/18-crown-6 recorded in CH_3CN. The peak at *m/z* 403.1 is assigned to [(BPMEN)Cr($^{14}NO_2^-$)(Cl^-)]$^+$ (calcd: *m/z* 403.1). The peaks at 387.1, 357.1, and 374.1 marked with asterisks are assigned to [(BPMEN)Cr(NO)(Cl^-)]$^+$ (calcd: *m/z* 387.1), [(BPMEN)Cr(Cl^-)]$^+$ (calcd: *m/z* 357.1) and [(BPMEN)Cr(OH^-)(Cl^-)]$^+$ (calcd: *m/z* 374.1), respectively. Inset: Isotopic distribution patterns of **4**-$^{14}NO_2^-$ (red line) and **4**-$^{15}NO_2^-$ (blue line).

sphere. It is worth noting that **2** does not show any spectral changes in the absence of $O_2^{\bullet-}$ under similar reaction conditions, suggesting that **2** is thermally stable; therefore, we can rule out the natural decomposition of **2** (ESI, Fig. S12b†).[51] In addition to the UV-vis spectral analysis, we investigated the NOO reaction of **2** with different spectral measurements and tried to follow or characterize the proposed [Cr–PN]$^+$ intermediate. However, being a thermally unstable species, our efforts to spectroscopically characterize the proposed [Cr–PN]$^+$ failed.

Further, to understand the NOO product of **2**, we characterized the reaction products with different spectral measurements. The FT-IR spectrum of the isolated product (**4**) from the reaction of **2** with $O_2^{\bullet-}$ showed a new peak at 1270 cm^{-1}, characteristic of NO_2^- stretching frequency (inset in Fig. 5a; ESI, Fig. S13a†).[19b] The NO_2^- stretching frequency shifted to 1243 cm^{-1} ($^{15}N^{16}O_2^-$) when reacting ^{15}NO-labeled **2** (*i.e.*, [(BPMEN)Cr(^{15}NO)(Cl^-)]$^+$) with $O_2^{\bullet-}$ (inset in Fig. 5b; ESI, Fig. S13b†). The negative shifting of NO_2^- stretching frequency (Δ = 27 cm^{-1}) denoted that the N atom in the NO_2^- anion came from the NO moiety of **2**. The ESI-MS spectrum of **4** exhibited a prominent ion peak at *m/z* 403.1, [(BPMEN)Cr^{III}(NO_2^-)(Cl^-)]$^+$ (calcd. *m/z* 403.1), which shifted to *m/z* 404.1, [(BPMEN)Cr^{III}($^{15}NO_2^-$)(Cl^-)]$^+$ (calcd. *m/z* 404.1), when the reaction was performed with ^{15}N-labeled **2** ($\{Cr^{15}NO\}^5$) (Fig. 5b; ESI, Fig. S14†), indicating clearly that the NO_2^- in **4** is derived from the NO moiety. Also, we compared the UV-vis spectrum of **4** with that of independently prepared Cr^{III}–NO_2^- (ESI, Fig. S15†), which further confirmed the formation of the Cr^{III}–NO_2^- complex in the NOO reaction of **2**. In addition, we calculated the magnetic moment of **4** by Evans' method and found it to be 3.54 BM (theoretical μ_s = 3.87 BM), confirming a Cr^{III} center (d^3) (ESI, Fig. S16†). Additionally, formation of **4** from the NOM reaction of **2** was also confirmed with EPR spectra as the spectrum of **4** showed a peak at g = 3.5 and 4.90 (ESI, Fig. S17†).[52] Cyclic voltammetric measurements of **4** showed a quasi-reversible cyclic voltammogram, clearly different from that of **2**, suggesting a completely new species (ESI, Fig. S16b and c†). For the exact validation of the NOO product of **2**, different spectroscopic data of an authentic sample of **4** were compared with those of the product obtained in the reaction of **2** with $O_2^{\bullet-}$. This comparison confirmed that the oxidized product of **2** is a Cr^{III}–metal complex bound to the NO_2^- anion.[19b] Complex **4** was found to be thermally stable, showing no natural decay in the UV-Vis measurements (ESI, Fig. S18a†). Finally, we determined the amount of NO_2^- ions by a Griess reagent assay[34a,47] in the reaction of **2** with NO and found it to be 87(±5)% (ESI, Fig. S10†). Various spectroscopic characterization studies of **4** showed that the reaction of $\{CrNO\}^5$ with $O_2^{\bullet-}$ yielded Cr^{III}–NO_2^- (**4**) as the NOM product (Scheme 3). Using a gas-mass analyzer we observed the formation of O_2 (ESI, Fig. S19b†).

Isomerization of the PN moiety is usually possible *via* O–O bond homolysis to form NO_3^-,[19c,20,41] or NO_2^- + O_2[48a,b,53] upon rearrangement. It is known that M–PN intermediates are highly unstable, and there are only a few reports on the spectral characterization of metal-bound PN intermediates.[19f,20,26b,54] However, alternatively, PN can also be confirmed using its phenol ring nitration chemistry when reacted with 2,4-DTBP *vide supra*.[19a–c,f,26b,40b,50a,54a,55] We observed the formation of NO_2-2,4-DTBP (yield: 65%) when **2** was reacted with $O_2^{\bullet-}$ in the presence of 2,4-DTBP (ESI, Fig. S20†). This phenol ring nitration test using 2,4-DTBP supports that the reaction of **1** with $O_2^{\bullet-}$ is going through a proposed [Cr–PN]$^+$ intermediate and generates Cr^{III}–NO_2^- + O_2 (Scheme 3).

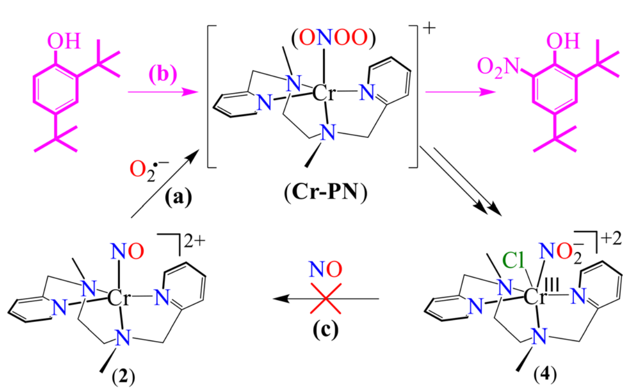

Scheme 3 Phenol ring nitration to trap the [Cr–PN]$^+$ intermediate.

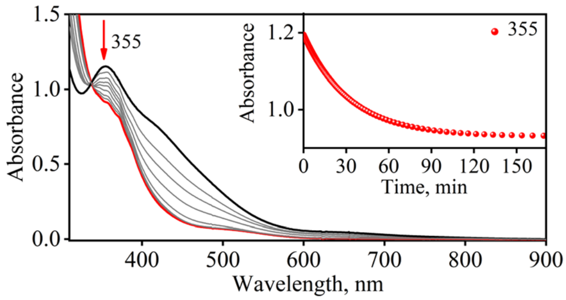

Fig. 6 UV-Vis spectral changes observed in the reaction of **3** (0.5 mM) with NO in CH_3CN under Ar at 233 K. Inset: Time course of decomposition of **3** monitored at 355 nm (red circles).

In addition, to determine the driving forces for the NOO reaction of **1** and **2**, the equilibrium constants (K_{eq}) for the formation of $\{CoNO\}^8$ and $\{CrNO\}^5$ were determined and found to be 88 M^{-1} and 2270 M^{-1} (ESI, Fig. S21a and b†), respectively, which suggest that the K_{eq} for **2** is ~25 times larger than that of **1**. This comparison of K_{eq} values undoubtedly suggests that $\{CrNO\}^5$ is more stable than $\{CoNO\}^8$. Hence, the NOO reaction of $\{CoNO\}^8$ was found to be faster than that of $\{CrNO\}^5$ in the presence of $O_2^{\bullet-}$.

NO activation of NOM products (3 and 4)

To further explore the chemistry of Co^{II}–NO_2^- (**3**) and Cr^{III}–NO_2^- (**4**) complexes, we investigated their reactions with excess NO. In this regard, we reacted isolated **3** (obtained in the reaction of **1** with one equivalent of $O_2^{\bullet-}$) with excess NO to explore its NO activation chemistry. In the reaction, we observed the decomposition of the band 355 nm and the formation of a new absorption band (λ_{max} = 375 nm) in ~2 hours in CH_3CN under an Ar atmosphere at 233 K, suggesting the generation of a new species, believed to be $\{CoNO\}^8$ (Fig. 6) (Scheme 2, step c). This indicates that complex **1** first reacts with one equivalent of $O_2^{\bullet-}$ to generate the corresponding Co^{II}–NO_2^-, which reacts further with NO to produce $\{CoNO\}^8$. In contrast to the NO activation of **3**, the reaction of **4** with excess NO did not yield Cr–NO, $[(BPMEN)Cr(NO)(Cl^-)]^+$ (**2**), under similar reaction conditions (Scheme 3, step d and ESI, Fig. S22†) which is so obvious as the end product of the NOO reaction is the Cr^{III} system. The exploration of the NO activation chemistry of Co^{II} (d^7, S = 3/2 or d^7, S = 1/2), Cr^{II} (d^4, S = 2), and Cr^{III} (d^3, S = 3/2) complexes with similar ligand frameworks suggests that M–nitrosyl formation depends on the oxidation states and physical parameters of the metal center.

Conclusion

In this report, we have demonstrated that the nitric oxide oxygenation (NOO) reactions of Co–nitrosyl, $[(BPMEN)Co(NO)]^{2+}$ ($\{CoNO\}^8$, **1**), and Cr–nitrosyl, $[(BPMEN)Cr(NO)(Cl^-)]^+$ ($\{CrNO\}^5$, **2**), complexes, bearing a common BPMEN ligand, are regulated by the stability of metal–nitrosyls and the intermediate species involved in the reactions. Here, we observed that the reaction of **1** with $O_2^{\bullet-}$ generates a Co^{II}–nitrite complex in the same oxidation state, $[(BPMEN)Co^{II}(NO_2^-)_2]$ (**3**), with O_2 evolution *via* a proposed $[Co–PN]^+$ intermediate, as observed in other examples of NOM chemistry.[22,24] In contrast, when **2** reacted with $O_2^{\bullet-}$, it generated an oxidized Cr^{III}–nitrite complex, $[(BPMEN)Cr^{III}(NO_2^-)Cl^-]^+$ (**4**), and O_2 *via* a putative $[Cr–PN]^+$ intermediate, similar to the chemistry of Co^{II}–PN and Cu^{II}–PN intermediates.[22,35a,49a] The proposed PN intermediates in the NOM reaction of **1** and **2** were supported by the phenol ring nitration test. Studies using ^{15}N-labeled ^{15}NO revealed that the N-atoms of Co^{II}–NO_2^- and Cr^{III}–NO_2^- derived from the NO moieties of **1** and **2**, respectively. Both the complexes, **1** and **2**, generate the NOM products (**3** and **4**) when reacted with $O_2^{\bullet-}$; however, we were only able to regenerate $\{CoNO\}^8$ from **3**, in contrast, $\{CrNO\}^5$ from **4**. In conclusion, the rate of NOM depends on the thermal stability of M–NOs. In contrast, the regeneration of initial M–NOs from NOM products depends on the oxidation states of the metal center of final products.

Conflicts of interest

There are no conflicts to declare.

Acknowledgements

This work was supported by Grants-in-Aid (Grant No. CRG/2021/003371 & EEQ/2021/000109) from SERB-DST. AK thanks the SERB-DST for her fellowship (Grant No. CRG/2021/003371). SD, K, and PB thank IISER, Tirupati, for their fellowships.

References

1 (*a*) G. B. Richter-Addo, P. Legzdins and J. Burstyn, *Chem. Rev.*, 2002, **102**, 857–860; (*b*) C. Bogdan, *Nat. Immunol.*, 2001, **2**, 907–916; (*c*) L. Jia, C. Bonaventura, J. Bonaventura and J. S. Stamler, *Nature*, 1996, **380**, 221–226.

2 (*a*) R. F. Furchgott, *Angew. Chem., Int. Ed.*, 1999, **38**, 1870–1880; (*b*) L. J. Ignarro, *Biosci. Rep.*, 1999, **19**, 51–71; (*c*) L. J. Ignarro, *Nitric Oxide: Biology and Pathobiology*, Academic press, 2000; (*d*) N. Lehnert, E. Kim, H. T. Dong, J. B. Harland, A. P. Hunt, E. C. Manickas, K. M. Oakley, J. Pham, G. C. Reed and V. S. Alfaro, *Chem. Rev.*, 2021, **121**(24), 14682–14905.

3 C. S. Wilcox, *Am. J. Physiol.: Regul., Integr. Comp. Physiol.*, 2005, **289**, R913–R935.

4 H. Li and U. Förstermann, *Curr. Opin. Pharmacol.*, 2013, **13**, 161–167.

5 C. Hölscher, L. McGlinchey, R. Anwyl and M. J. Rowan, *Learn. Mem.*, 1996, **2**, 267–278.

6 (*a*) F. Vargas, J. M. Moreno, R. Wangensteen, I. Rodriguez-Gomez and J. Garcia-Estan, *Eur. J. Endocrinol.*, 2007, **156**,

1–12; (*b*) S. Cook, O. Hugli, M. Egli, P. Vollenweider, R. Burcelin, P. Nicod, B. Thorens and U. Scherrer, *Swiss Med. Wkly.*, 2003, **133**, 360–363.
7 (*a*) L. Castillo, T. C. deRojas, T. E. Chapman, J. Vogt, J. F. Burke, S. R. Tannenbaum and V. R. Young, *Proc. Natl. Acad. Sci. U. S. A.*, 1993, **90**, 193–197; (*b*) R. M. Palmer, D. S. Ashton and S. Moncada, *Nature*, 1988, **333**, 664–666.
8 (*a*) Q. Liu and S. S. Gross, *Methods Enzymol.*, 1996, **268**, 311–324; (*b*) C. Nathan and Q. W. Xie, *J. Biol. Chem.*, 1994, **269**, 13725–13728.
9 (*a*) B. A. Averill, *Chem. Rev.*, 1996, **96**, 2951–2964; (*b*) J. O. Lundberg, E. Weitzberg and M. T. Gladwin, *Nat. Rev. Drug Discovery*, 2008, **7**, 156–167.
10 R. Radi, *Proc. Natl. Acad. Sci. U. S. A.*, 2004, **101**, 4003–4008.
11 C. H. Lim, P. C. Dedon and W. M. Deen, *Chem. Res. Toxicol.*, 2008, **21**, 2134–2147.
12 R. S. Lewis and W. M. Deen, *Chem. Res. Toxicol.*, 1994, **7**, 568–574.
13 (*a*) S. Goldstein, J. Lind and G. Merenyi, *Chem. Rev.*, 2005, **105**, 2457–2470; (*b*) P. C. Dedon and S. R. Tannenbaum, *Arch. Biochem. Biophys.*, 2004, **423**, 12–22; (*c*) P. Pacher, J. S. Beckman and L. Liaudet, *Physiol. Rev.*, 2007, **87**, 315–424.
14 B. Kalyanaraman, *Proc. Natl. Acad. Sci. U. S. A.*, 2004, **101**, 11527–11528.
15 (*a*) P. R. Gardner, A. M. Gardner, L. A. Martin and A. L. Salzman, *Proc. Natl. Acad. Sci. U. S. A.*, 1998, **95**, 10378–10383; (*b*) M. P. Doyle and J. W. Hoekstra, *J. Inorg. Biochem.*, 1981, **14**, 351–358; (*c*) P. C. Ford and I. M. Lorkovic, *Chem. Rev.*, 2002, **102**, 993–1018.
16 D. A. Nnate and N. K. Achi, *J. Sci. Res. Rep.*, 2016, **1**, 1–19.
17 (*a*) N. Pal, M. Jana and A. Majumdar, *Chem. Commun.*, 2021, **57**, 8682–8698; (*b*) P. C. Mills, G. Rowley, S. Spiro, J. C. D. Hinton and D. J. Richardson, *Microbiology-SGM*, 2008, **154**, 1218–1228; (*c*) A. M. Gardner, R. A. Helmick and P. R. Gardner, *J. Biol. Chem.*, 2002, **277**, 8172–8177.
18 (*a*) R. F. Eich, T. Li, D. D. Lemon, D. H. Doherty, S. R. Curry, J. F. Aitken, A. J. Mathews, K. A. Johnson, R. D. Smith, G. N. Phillips and J. S. Olson, *Biochemistry*, 1996, **35**, 6976–6983; (*b*) R. E. Huie and S. Padmaja, *Free Radical Res. Commun.*, 1993, **18**, 195–199; (*c*) S. Herold, *FEBS Lett.*, 1999, **443**, 81–84.
19 (*a*) A. Yokoyama, J. E. Han, K. D. Karlin and W. Nam, *Chem. Commun.*, 2014, **50**, 1742–1744; (*b*) A. Yokoyama, K. B. Cho, K. D. Karlin and W. Nam, *J. Am. Chem. Soc.*, 2013, **135**, 14900–14903; (*c*) A. Yokoyama, J. E. Han, J. Cho, M. Kubo, T. Ogura, M. A. Siegler, K. D. Karlin and W. Nam, *J. Am. Chem. Soc.*, 2012, **134**, 15269–15272; (*d*) T. S. Kurtikyan, S. R. Eksuzyan, J. A. Goodwin and G. S. Hovhannisyan, *Inorg. Chem.*, 2013, **52**, 12046–12056; (*e*) T. S. Kurtikyan and P. C. Ford, *Chem. Commun.*, 2010, **46**, 8570–8572; (*f*) S. K. Sharma, A. W. Schaefer, H. Lim, H. Matsumura, P. Moënne-Loccoz, B. Hedman, K. O. Hodgson, E. I. Solomon and K. D. Karlin, *J. Am. Chem. Soc.*, 2017, **139**, 17421–17430; (*g*) S. K. Sharma, P. J. Rogler and K. D. Karlin, *J. Porphyrins Phthalocyanines*, 2015, **19**, 352–360.
20 T. S. Kurtikyan, S. R. Eksuzyan, V. A. Hayrapetyan, G. G. Martirosyan, G. S. Hovhannisyan and J. A. Goodwin, *J. Am. Chem. Soc.*, 2012, **134**, 13861–13870.
21 S. Saha, S. Ghosh, K. Gogoi, H. Deka, B. Mondal and B. Mondal, *Inorg. Chem.*, 2017, **56**, 10932–10938.
22 D. Maiti, D. H. Lee, A. A. Narducci Sarjeant, M. Y. Pau, E. I. Solomon, K. Gaoutchenova, J. Sundermeyer and K. D. Karlin, *J. Am. Chem. Soc.*, 2008, **130**, 6700–6701.
23 S. Hong, P. Kumar, K. B. Cho, Y. M. Lee, K. D. Karlin and W. Nam, *Angew. Chem., Int. Ed.*, 2016, **55**, 12403–12407.
24 M. Yenuganti, S. Das, Kulbir, S. Ghosh, P. Bhardwaj, S. S. Pawar, S. C. Sahoo and P. Kumar, *Inorg. Chem. Front.*, 2020, **7**, 4872–4882.
25 (*a*) J. Lee, J. A. Hunt and J. T. Groves, *J. Am. Chem. Soc.*, 1998, **120**, 7493–7501; (*b*) J. Su and J. T. Groves, *J. Am. Chem. Soc.*, 2009, **131**, 12979–12988.
26 (*a*) J. J. Liu, M. A. Siegler, K. D. Karlin and P. Moenne-Loccoz, *Angew. Chem., Int. Ed.*, 2019, **58**, 10936–10940; (*b*) N. G. Tran, H. Kalyvas, K. M. Skodje, T. Hayashi, P. Moënne-Loccoz, P. E. Callan, J. Shearer, L. J. Kirschenbaum and E. Kim, *J. Am. Chem. Soc.*, 2011, **133**, 1184–1187.
27 K. J. Koebke, D. J. Pauly, L. Lerner, X. Liu and A. A. Pacheco, *Inorg. Chem.*, 2013, **52**, 7623–7632.
28 E. T. Yukl, S. de Vries and P. Moënne-Loccoz, *J. Am. Chem. Soc.*, 2009, **131**, 7234–7235.
29 (*a*) M. T. Forrester and M. W. Foster, *Free Radicals Biol. Med.*, 2012, **52**, 1620–1633; (*b*) P. Ascenzi and M. Brunori, *J. Porphyrins Phthalocyanines*, 2016, **20**, 134–149.
30 J. Tejero, A. P. Hunt, J. Santolini, N. Lehnert and D. J. Stuehr, *J. Biol. Chem.*, 2019, **294**, 7904–7916.
31 (*a*) G. B. Richter-Addo and P. Legzdins, *Metal nitrosyls*, Oxford University Press, 1992; (*b*) S. Hematian, I. Garcia-Bosch and K. D. Karlin, *Acc. Chem. Res.*, 2015, **48**, 2462–2474; (*c*) J. Fitzpatrick and E. Kim, *Acc. Chem. Res.*, 2015, **48**, 2453–2461; (*d*) A. P. Hunt and N. Lehnert, *Acc. Chem. Res.*, 2015, **48**, 2117–2125; (*e*) M.-L. Tsai, C.-C. Tsou and W.-F. Liaw, *Acc. Chem. Res.*, 2015, **48**, 1184–1193; (*f*) T. C. Berto, A. L. Speelman, S. Zheng and N. Lehnert, *Coord. Chem. Rev.*, 2013, **257**, 244–259; (*g*) M. Sarma, A. Kalita, P. Kumar, A. Singh and B. Mondal, *J. Am. Chem. Soc.*, 2010, **132**, 7846–7847; (*h*) P. Kumar, A. Kalita and B. Mondal, *Dalton Trans.*, 2011, **40**, 8656–8663; (*i*) A. Kalita, P. Kumar, R. C. Deka and B. Mondal, *Inorg. Chem.*, 2011, **50**, 11868–11876; (*j*) B. Mondal, P. Kumar, P. Ghosh and A. Kalita, *Chem. Commun.*, 2011, **47**, 2964–2966.
32 A. Boscari, E. Meilhoc, C. Castella, C. Bruand, A. Puppo and R. Brouquisse, *Front. Plant Sci.*, 2013, **4**, 384.
33 (*a*) C. E. Sparacino-Watkins, J. Tejero, B. Sun, M. C. Gauthier, J. Thomas, V. Ragireddy, B. A. Merchant, J. Wang, I. Azarov, P. Basu and M. T. Gladwin, *J. Biol. Chem.*, 2014, **289**, 10345–10358; (*b*) C. Gherasim, P. K. Yadav, O. Kabil, W. N. Niu and R. Banerjee, *PLoS One*, 2014, **9**, e85544; (*c*) J. L. Zweier, P. Wang, A. Samouilov and P. Kuppusamy, *Nat. Med.*, 1995, **1**, 804–809; (*d*) Kulbir, S. Das, T. Devi, S. Ghosh, S. Chandra Sahoo and P. Kumar,

Chem. Sci., 2023, **14**, 2935–2942; (*e*) Kulbir, S. Das, T. Devi, M. Goswami, M. Yenuganti, P. Bhardwaj, S. Ghosh, S. C. Sahoo and P. Kumar, *Chem. Sci.*, 2021, **12**, 10605–10612.

34 (*a*) H. Subedi and N. E. Brasch, *Inorg. Chem.*, 2013, **52**, 11608–11617; (*b*) C. M. Frech, O. Blacque, H. W. Schmalle and H. Berke, *Dalton Trans.*, 2006, 4590–4598, DOI: 10.1039/B604858G.

35 (*a*) P. Kumar, Y. M. Lee, Y. J. Park, M. A. Siegler, K. D. Karlin and W. Nam, *J. Am. Chem. Soc.*, 2015, **137**, 4284–4287; (*b*) P. Kumar, Y. M. Lee, L. Hu, J. Chen, Y. J. Park, J. Yao, H. Chen, K. D. Karlin and W. Nam, *J. Am. Chem. Soc.*, 2016, **138**, 7753–7762; (*c*) M. A. Puthiyaveetil Yoosaf, S. Ghosh, Y. Narayan, M. Yadav, S. C. Sahoo and P. Kumar, *Dalton Trans.*, 2019, **48**, 13916–13920; (*d*) S. Das, S. A. C. Kulbir, S. Singh, S. Roy, R. Singh, S. Ghosh and P. Kumar, *Dalton Trans.*, 2023, **52**, 5095; (*e*) A. Kalita, P. Kumar, R. C. Deka and B. Mondal, *Chem. Commun.*, 2012, **48**, 1251–1253; (*f*) A. Kalita, P. Kumar and B. Mondal, *Chem. Commun.*, 2012, **48**, 4636–4638; (*g*) P. Kumar, A. Kalita and B. Mondal, *Inorg. Chim. Acta*, 2013, **404**, 88–96; (*h*) P. Kumar, A. Kalita and B. Mondal, *Dalton Trans.*, 2012, **41**, 10543–10548; (*i*) P. Kumar, A. Kalita and B. Mondal, *Dalton Trans.*, 2011, **40**, 8656–8663.

36 (*a*) S. Das, Kulbir, S. Ghosh, S. Chandra Sahoo and P. Kumar, *Chem. Sci.*, 2020, **11**, 5037–5042; (*b*) F. Roncaroli, J. A. Olabe and R. van Eldik, *Inorg. Chem.*, 2002, **41**, 5417–5425.

37 A. Kalita, P. Kumar, R. C. Deka and B. Mondal, *Chem. Commun.*, 2012, **48**, 1251–1253.

38 (*a*) S. G. Clarkson and F. Basolo, *J. Chem. Soc., Chem. Commun.*, 1972, 670–671, DOI: 10.1039/c39720000670; (*b*) S. G. Clarkson and F. Basolo, *Inorg. Chem.*, 1973, **12**, 1528–1534.

39 L. Cheng, D. R. Powell, M. A. Khan and G. B. Richter-Addo, *Chem. Commun.*, 2000, 2301–2302, DOI: 10.1039/b006775j.

40 (*a*) B. Mondal, S. Saha, D. Borah, R. Mazumdar and B. Mondal, *Inorg. Chem.*, 2019, **58**, 1234–1240; (*b*) A. Kalita, P. Kumar and B. Mondal, *Chem. Commun.*, 2012, **48**, 4636–4638.

41 B. Mondal, D. Borah, R. Mazumdar and B. Mondal, *Inorg. Chem.*, 2019, **58**, 14701–14707.

42 (*a*) C. P. Brock, J. P. Collman, G. Dolcetti, P. H. Farnham, J. A. Ibers, J. E. Lester and C. A. Reed, *Inorg. Chem.*, 2002, **12**, 1304–1313; (*b*) C. H. Chuang, W. F. Liaw and C. H. Hung, *Angew. Chem., Int. Ed.*, 2016, **55**, 5190–5194; (*c*) K. Gogoi, S. Saha, B. Mondal, H. Deka, S. Ghosh and B. Mondal, *Inorg. Chem.*, 2017, **56**, 14438–14445; (*d*) Y. Guo, J. R. Stroka, B. Kandemir, C. E. Dickerson and K. L. Bren, *J. Am. Chem. Soc.*, 2018, **140**, 16888–16892; (*e*) H. Kruszyna, J. S. Magyar, L. G. Rochelle, M. A. Russell, R. P. Smith and D. E. Wilcox, *J. Pharmacol. Exp. Ther.*, 1998, **285**, 665–671; (*f*) A. Keller, Jeż and B. Owska-Trzebiatowska, *Inorg. Chim. Acta*, 1981, **51**, 123–130; (*g*) A. Døssing, *Rev. Inorg. Chem.*, 2013, **33**, 129–137.

43 S. Das, Kulbir, S. Ray, T. Devi, S. Ghosh, S. S. Harmalkar, S. N. Dhuri, P. Mondal and P. Kumar, *Chem. Sci.*, 2022, **13**, 1706–1714.

44 Kulbir, C. S. A. Keerthi, S. Beegam, S. Das, P. Bhardwaj, M. Ansari, K. Singh and P. Kumar, *Inorg. Chem.*, 2023, **62**, 7385–7392.

45 (*a*) J. Cho, H. Y. Kang, L. V. Liu, R. Sarangi, E. I. Solomon and W. Nam, *Chem. Sci.*, 2013, **4**, 1502–1508; (*b*) J. Du, D. Xu, C. Zhang, C. Xia, Y. Wang and W. Sun, *Dalton Trans.*, 2016, **45**, 10131–10135; (*c*) Y. Jo, J. Annaraj, M. S. Seo, Y.-M. Lee, S. Y. Kim, J. Cho and W. Nam, *J. Inorg. Biochem.*, 2008, **102**, 2155–2159.

46 D. F. Evans, *J. Chem. Soc.*, 1959, 2003–2005, DOI: 10.1039/jr9590002003.

47 E. Tatsch, G. V. Bochi, R. D. S. Pereira, H. Kober, V. A. Agertt, M. M. Anraku de Campos, P. Gomes, M. M. M. F. Duarte and R. N. Moresco, *Clin. Biochem.*, 2011, **44**, 348–350.

48 (*a*) J. W. Coddington, J. K. Hurst and S. V. Lymar, *J. Am. Chem. Soc.*, 1999, **121**, 2438–2443; (*b*) S. Pfeiffer, A. C. Gorren, K. Schmidt, E. R. Werner, B. Hansert, D. S. Bohle and B. Mayer, *J. Biol. Chem.*, 1997, **272**, 3465–3470.

49 (*a*) G. Y. Park, S. Deepalatha, S. C. Puiu, D. H. Lee, B. Mondal, A. A. Narducci Sarjeant, D. del Rio, M. Y. Pau, E. I. Solomon and K. D. Karlin, *J. Biol. Inorg. Chem.*, 2009, **14**, 1301–1311; (*b*) O. A. Babich and E. S. Gould, *Res. Chem. Intermed.*, 2002, **28**, 575–583.

50 (*a*) R. Cao, L. T. Elrod, R. L. Lehane, E. Kim and K. D. Karlin, *J. Am. Chem. Soc.*, 2016, **138**, 16148–16158; (*b*) R. Mazumdar, B. Mondal, S. Saha, B. Samanta and B. Mondal, *J. Inorg. Biochem.*, 2022, **228**, 111698.

51 J. Cho, R. Sarangi, J. Annaraj, S. Y. Kim, M. Kubo, T. Ogura, E. I. Solomon and W. Nam, *Nat. Chem.*, 2009, **1**, 568–572.

52 S. Das, Kulbir, S. Ray, T. Devi, S. Ghosh, S. S. Harmalkar, S. N. Dhuri, P. Mondal and P. Kumar, *Chem. Sci.*, 2022, **13**, 1706–1714.

53 W. H. Koppenol, P. L. Bounds, T. Nauser, R. Kissner and H. Ruegger, *Dalton Trans.*, 2012, **41**, 13779–13787.

54 (*a*) M. P. Schopfer, B. Mondal, D. H. Lee, A. A. Sarjeant and K. D. Karlin, *J. Am. Chem. Soc.*, 2009, **131**, 11304–11305; (*b*) J. J. Liu, M. A. Siegler, K. D. Karlin and P. Moenne-Loccoz, *Angew. Chem., Int. Ed.*, 2019, **58**, 10936–10940.

55 (*a*) M. S. Ramezanian, S. Padmaja and W. H. Koppenol, *Chem. Res. Toxicol.*, 1996, **9**, 232–240; (*b*) A. Vandervliet, J. P. Eiserich, C. A. Oneill, B. Halliwell and C. E. Cross, *Arch. Biochem. Biophys.*, 1995, **319**, 341–349; (*c*) A. van der Vliet, C. A. O'Neill, B. Halliwell, C. E. Cross and H. Kaur, *FEBS Lett.*, 1994, **339**, 89–92; (*d*) A. Kalita, R. C. Deka and B. Mondal, *Inorg. Chem.*, 2013, **52**, 10897–10903; (*e*) S. Kim, M. A. Siegler and K. D. Karlin, *Chem. Commun.*, 2014, **50**, 2844–2846; (*f*) L. Qiao, Y. Lu, B. Liu and H. H. Girault, *J. Am. Chem. Soc.*, 2011, **133**, 19823–19831; (*g*) K. M. Skodje, P. G. Williard and E. Kim, *Dalton Trans.*, 2012, **41**, 7849–7851.